J|A|C|S
ARTICLES
Published on Web 03/05/2002

Structural Characterization of Metallopeptides Designed as Scaffolds for the Stabilization of Nickel(II)-Fe_4S_4 Bridged Assemblies by X-ray Absorption Spectroscopy

Kristin B. Musgrave,[†] Catalina E. Laplaza,[‡] R. H. Holm,*[,‡] Britt Hedman,[†,§,*] and Keith O. Hodgson*[,†,§]

Contribution from the Department of Chemistry, Stanford University, Stanford, California 94305, Stanford Synchrotron Radiation Laboratory, SLAC, Stanford University, Stanford, California 94309, and the Department of Chemistry and Chemical Biology, Harvard University, Cambridge, Massachusetts 02138

Received July 31, 2001

Abstract: In earlier work, *de novo* designed peptides with a helix−loop−helix motif and 63 residues have been synthesized as potential scaffolds for stabilization of the [Ni^{II}-X-Fe_4S_4] bridged assembly that is the spectroscopically deduced structure of the A-Cluster in clostridial carbon monoxide dehydrogenase. The 63mers contain a consensus tricysteinyl ferredoxin domain in the loop for binding an Fe_4S_4 cluster and Cys and His residues proximate to the loop for binding Ni(II), with one Cys residue designed as the bridge X. The metallopeptides HC_4H_2-[Fe_4S_4]-Ni and HC_5H-[Fe_4S_4]-M, containing three His and one Cys residue for Ni(II) coordination and two His and two Cys residues for binding M = Ni(II) and Co(II), have been examined by Fe-, Ni-, and Co-K edge spectroscopy and EXAFS. All peptides bind an $[Fe_4S_4]^{2+}$ cubane-type cluster. Interpretation of the Ni and Co data is complicated by the presence of a minority population of six-coordinate species with low Z ligands, designated for simplicity as $[M(OH_2)_6]^{2+}$. Best fits of the data were obtained with ca. 20% $[M(OH_2)_6]^{2+}$ and ca. 80% M(II) with mixed N/S coordination. The collective XAS results for HC_4H_2-[Fe_4S_4]-Ni and HC_5H-[Fe_4S_4]-M demonstrate the presence of an Fe_4S_4 cluster and support the existence of the distorted square-planar coordination units [Ni^{II}(S·Cys)(N·His)$_3$] and [Ni^{II}(S·Cys)$_2$-(N·His)$_2$] in the HC_4H_2 and HC_5H metallopeptides, respectively. In the HC_5H metallopeptide, tetrahedral [Co^{II}(S·Cys)$_2$(N·His)$_2$] is present. We conclude that the designed scaffolded binding sites, including Ni-(μ_2-S·Cys)-Fe bridges, have been achieved. This is the first XAS study of a *de novo* designed metallopeptide intended to stabilize a bridged biological assembly, and one of a few XAS analyses of metal derivatives of designed peptides. The scaffolding concept should be extendable to other bridged metal assemblies.

Introduction

De novo designed peptides are increasingly employed to simulate metal binding sites in native proteins.[1] Prominent examples include metallopeptides pertinent to zinc fingers,[2,3] rubredoxins,[4,5] ferredoxins,[6−14] heme proteins,[15] and diiron proteins.[16,17] We are interested in the use of designed peptides as scaffolds for the stabilization of complex metal sites in proteins that we have described as bridged assemblies in which two fragments of the site are connected by one or more covalent bridges.[18] In this context, we[19] have recently prepared helix−loop−helix peptides designed for the encapsulation and stabilization of a bridged structure [Ni-X-Fe_4S_4] that has been proposed for the A-Cluster of the nickel-containing enzyme carbon monoxide dehydrogenase (CODH).[20] This center is the site of catalysis of the last step in the synthesis of acetyl-CoA from carbon monoxide, coenzyme A, and a methyl group from

[†] Stanford University.
[‡] Harvard University.
[§] Stanford Synchrotron Radiation Laboratory

(1) DeGrado, W. F.; Summa, C. M.; Pavone, V.; Nastri, F.; Lombardi, A. *Annu. Rev. Biochem.* **1999**, *68*, 779−819.
(2) Berg, J. M.; Godwin, H. A. *Annu. Rev. Biophys. Biomol. Struct.* **1997**, *26*, 357−371.
(3) Blasie, C. A.; Berg, J. M. *Inorg. Chem.* **2000**, *39*, 348−351.
(4) Low, D. W.; Hill, M. G. *J. Am. Chem. Soc.* **1998**, *120*, 11536−11537.
(5) Lombardi, A.; Marasco, D.; Maglio, O.; Di Costanzo, L.; Nastri, F.; Pavone, V. *Proc. Natl. Acad. Sci. U.S.A.* **2000**, *97*, 11922−11927.
(6) Smith, E. T.; Feinberg, B. A.; Richards, J. H.; Tomich, J. M. *J. Am. Chem. Soc.* **1991**, *113*, 688−689.
(7) Smith, E. T.; Tomich, J. M.; Iwamoto, T.; Richards, J. H.; Mao, Y.; Feinberg, B. A. *Biochemistry* **1991**, *30*, 11669−11676.
(8) Sow, T.-C.; Pedersen, M. V.; Christensen, H. E. M.; Ooi, B.-L. *Biochem. Biophys. Res. Commun.* **1996**, *223*, 360−364.
(9) Gibney, B. R.; Mulholland, S. E.; Rabanal, F.; Dutton, P. L. *Proc. Natl. Acad. Sci. U.S.A.* **1996**, *93*, 15041−15046.
(10) Feinberg, B. A.; Lo, X.; Iwamoto, T.; Tomich, J. M. *Protein Eng.* **1997**, *10*, 69−75.
(11) Scott, M. P.; Biggins, J. *Protein Sci.* **1997**, *6*, 340−346.
(12) Coldren, C. D.; Hellinga, H. W.; Caradonna, J. P. *Proc. Natl. Acad. Sci. U.S.A.* **1997**, *94*, 6635−6640.
(13) Mulholland, S. E.; Gibney, B. R.; Rabanal, F.; Dutton, P. L. *J. Am. Chem. Soc.* **1998**, *120*, 10296−10302.
(14) Mulholland, S. E.; Gibney, B. R.; Rabanal, F.; Dutton, P. L. *Biochemistry* **1999**, *38*, 10442−10448.
(15) Gibney, B. R.; Dutton, P. L. *Adv. Inorg. Chem.* **2001**, *51*, 409−455.
(16) Lombardi, A.; Summa, C. M.; Geremia, S.; Randaccio, L.; Pavone, V.; DeGrado, W. F. *Proc. Natl. Acad. Sci. U.S.A.* **2000**, *97*, 6298−6305.
(17) Pasternak, A.; Kaplan, J.; Lear, J. D.; DeGrado, W. F. *Protein Sci.* **2001**, *10*, 958−969.
(18) Holm, R. H. *Pure Appl. Chem.* **1995**, *67*, 217−224.
(19) Laplaza, C. E.; Holm, R. H. *J. Am. Chem. Soc.* **2001**, *123*, 10255−10264.
(20) Ragsdale, S. W.; Kumar, M. *Chem. Rev.* **1996**, *96*, 2515−2539.

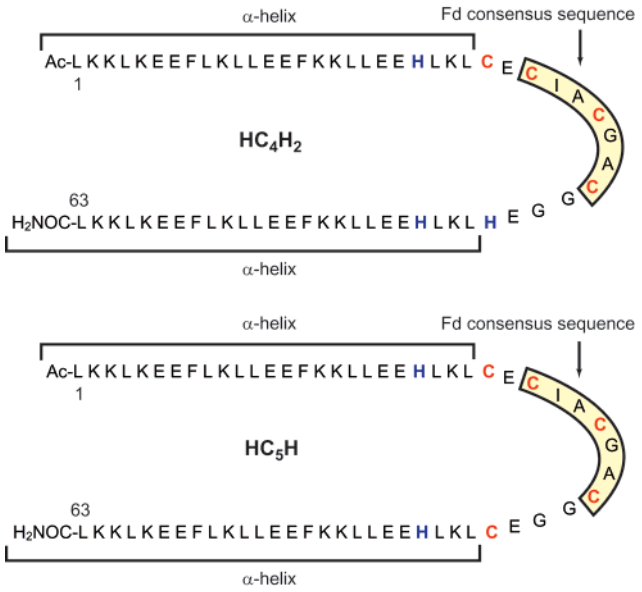

Figure 1. Amino acid sequences of the 63mers HC_4H_2 and HC_5H.

a methylated corrinoid iron−sulfur protein. From spectroscopic evidence, Ni(II) has been postulated to be linked to an iron atom of an Fe_4S_4 cluster through an unknown bridging ligand, and to be coordinated to 2 S ligands and 2 N/O ligands in a distorted square-planar geometry.[21,22] Such a [Ni-X-Fe_4S_4] bridged arrangement has been difficult to stabilize with conventional ligands. The only examples of complexes with Ni(II) ligated to an Fe_4S_4 cluster are $[\{Ni(EtN_2S_2)\}_2Fe_4S_4I_2]$,[23] $[\{Ni(EtN_2S_2)\}_2Fe_4S_4(Stip)_2]$,[23] and $[Ni(EtN_2S_2)Fe_4S_4I_3]^{1-}$ [24] (EtN_2S_2 = *N*,*N*′-diethyl-3,7-diazanonane-1,9-dithiolate(2−); Stip = 2,4,6-triisopropylbenzenethiolate(1−)). From these, only the last complex contains the enzyme stoichiometry of one nickel atom per Fe_4S_4 cluster. Furthermore, when the above complexes are in solution, each nickel ion is covalently linked to the cluster by two, rather than one, thiolate bridges.

Efforts in this laboratory are directed toward the design of peptides that can scaffold bridged metal assemblies. For the encapsulation of the A-Cluster of CODH, several 63mer peptides, two of which are shown in Figure 1, were designed such that two long α-helices are linked by a loop containing the ferredoxin consensus sequence **Cys**-Ile-Ala-**Cys**-Gly-Ala-**Cys** for the binding of the Fe_4S_4 cluster. A fourth cysteine, designed as the bridging ligand, and three other binding residues (histidines and cysteines) were placed close to the loop in optimal positions for the coordination of Ni(II). Two of the resulting metallopeptides, designated as HC_4H_2-[Fe_4S_4]-Ni and HC_5H-[Fe_4S_4]-Ni according to their cysteine and histidine content, were shown by absorption and Mössbauer spectroscopies to have peptide-bound $[Fe_4S_4]^{2+}$. Incubation of these peptides with a Ni(II) source followed by column chromatographic purification afforded metallopeptides containing the cluster and coordinated Ni(II). Binding of Ni(II) has been demonstrated by atomic absorption spectroscopy and difference absorption spectra of the Ni(II) reaction product and the Ni(II)-free peptide, both containing the Fe_4S_4 cluster.[19] The difference spectra suggest that in both peptides Ni(II) is coordinated in a planar or distorted planar arrangement with at least one cysteinate ligand. The overall structural motif of the peptides resembles the maquettes introduced by Gibney et al.[9] which were successfully designed to bind an Fe_4S_4 cluster and heme groups (through His residues) in the same metallopeptide molecule.

Among *de novo* designed peptides with biologically relevant metals, only the dizinc four-helix bundle prepared by DeGrado and co-workers[16] has been characterized by X-ray crystallography. A very few metallopeptides, such as the tetracysteinyl cyclopeptide Ni(II), Co(II), and Fe(II) complexes prepared in this laboratory,[25] have been analyzed by X-ray absorption spectroscopy (XAS). Structural characterization of metal sites of designed peptides is desirable not only because it provides strong evidence of where and how the metal binds, but also because it can provide information on the role that protein structure plays on the coordination geometry and ligand environment of the metal. As unusual coordination properties may be required to obtain function, the latter can be useful information for the development of functional analogues, and thereafter for the understanding of structure−function relationships.

To provide metal site structural characterization of our helix−loop−helix metallopeptides,[19] we have carried out a detailed XAS study of HC_4H_2-[Fe_4S_4]-Ni and HC_5H-[Fe_4S_4]-Ni and also of HC_5H-[Fe_4S_4]-Co. We report the results from analysis of Fe, Ni, and Co K-edge spectra and EXAFS. This study serves to corroborate the desired target metallopeptide structures shown in Figure 2 and constitutes one of the few reports of XAS applied to *de novo* designed metallopeptides. Detailed characterization of the peptides themselves and other properties of their metal derivatives have been presented earlier.[19]

Experimental Section

Preparation of Compounds. (a) Metallopeptides. The 63mer peptides HC_4H_2 and HC_5H and their derivatives containing one $[Fe_4S_4]^{2+}$ cluster and coordinated Ni(II) were prepared and purified as described elsewhere.[19] HC_5H-[Fe_4S_4]-Co was prepared and purified in an analogous manner. Metal ions were introduced using the reagents $[Ni(OH_2)_6]X_2$ (X = Cl^-, BF_4^-) and $[Co(OH_2)_6](BF_4)_2$. These species are designated as indicated below, together with their metal content as determined by atomic absorption spectroscopy. The sample with 1.0 Ni/4Fe was not chromatographed. All other samples were purified by chromatography on Sephadex G-25, a treatment that resulted in the loss of some Ni(II) or Co(II).

$$HC_4H_2\text{-}[Fe_4S_4]\text{-}Ni;\ 0.6-1.0\ Ni/4Fe$$

$$HC_5H\text{-}[Fe_4S_4]\text{-}M\ (M = Ni^{2+}, Co^{2+});\ 0.7\ M/4Fe$$

(b) Model Compounds. Certain complexes with structurally defined coordination units were required for comparison of their XAS properties with those of the metallopeptides. Complexes with planar NiN_3S[26,27] and NiN_2S_2[28] and tetrahedral CoN_2S_2[29] units, depicted in Figures 5 and 11, were prepared by literature methods.

XAS Sample Preparation, Data Collection, and Reduction. Lyophilized metallopeptide samples were loaded into 1 mm Lucite cells

(21) Xia, J.; Dong, J.; Wang, S.; Scott, R. A.; Lindahl, P. A. *J. Am. Chem. Soc.* **1995**, *117*, 7065−7070.
(22) Russell, W. K.; Stålhandske, C. M. V.; Xia, J.; Scott, R. A.; Lindahl, P. A. *J. Am. Chem. Soc.* **1998**, *120*, 7502−7510.
(23) Osterloh, F.; Saak, W.; Pohl, S. *J. Am. Chem. Soc.* **1997**, *119*, 5648−5656.
(24) Osterloh, F.; Saak, W.; Haase, D.; Pohl, S. *Chem. Commun.* **1996**, 777−778.
(25) Nivorozhkin, A. L.; Segal, B. M.; Musgrave, K. B.; Kates, S. A.; Hedman, B.; Hodgson, K. O.; Holm, R. H. *Inorg. Chem.* **2000**, *39*, 2306−2313.

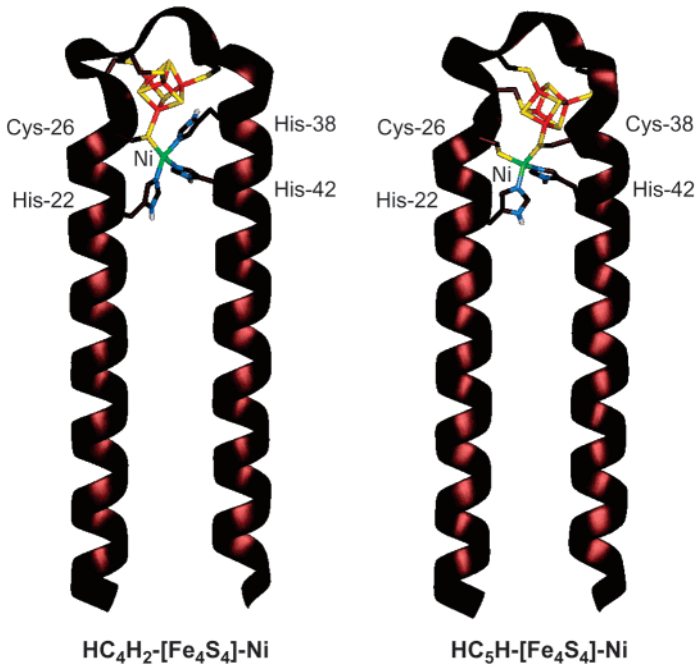

Figure 2. QUANTA models of the target metallopeptides HC_4H_2-[Fe_4S_4]-Ni and HC_5H-[Fe_4S_4]-Ni. The metal structures shown are supported by Fe and Ni K-edge and EXAFS analysis.

with 63.5 μm Kapton windows in an inert atmosphere (dinitrogen) glovebox. Air-sensitive, solid model complexes were ground into a fine powder in an inert atmosphere (dinitrogen) glovebox and diluted with boron nitride to maintain $\Delta\mu x \leq 1$ and prevent self-absorption. The mixture was pressed into a pellet and sealed between 63.5 μm Mylar tape windows in a 1 mm aluminum spacer. All air-sensitive samples were frozen in liquid nitrogen immediately upon removal from the glovebox and maintained at this or a lower temperature throughout storage and data collection. Air-stable, model complex samples were prepared in an analogous manner; however, manipulations were performed in air. Iron and nickel K-edge XAS data were measured for the preceding samples. The data for the various HC_4H_2-[Fe_4S_4]-Ni samples of different nickel content were superimposable and were independent of counterion X of the Ni(II) reactant. Data for a sample with a Ni:4Fe ratio of 0.8 are reported.

For all metallopeptide samples, XAS data were measured at the Stanford Synchrotron Radiation Laboratory (SSRL) on unfocused 8-pole wiggler beam line 7-3 and focused 16-pole wiggler beam line 9-3 under ring conditions 3.0 GeV, 70−100 mA. A Si(220) double crystal monochromator was utilized for energy selection at the respective edges (Fe, Co, and Ni K-edges). For data measured on beam line 7-3, the monochromator was detuned 50% at 8257 (Fe K-edge), 8831 (Co K-edge), and 9439 eV (Ni K-edge) to minimize contamination from higher harmonics; for beam line 9-3, a harmonic rejection mirror was used and the monochromator was fully tuned. An Oxford Instruments CF1208 continuous flow liquid helium cryostat was used to maintain a constant sample temperature of 10 K. Data were measured in fluorescence mode using a 13-element (beam line 7-3) or 30-element (beam line 9-3) Ge array detector,[30] to $k = 17$ Å^{-1} (Fe and Co K-edges), and $k = 16$ Å^{-1} (Ni K-edge). Internal calibration was performed by simultaneous measurement of absorption edges of the corresponding elemental foil placed between a second and third ionization chamber. The first inflection point of the Fe, Co, and Ni foil spectra was assigned to 7111.2, 7709.5, and 8331.6 eV, respectively. The XAS data for the model complexes were measured in transmission mode under similar conditions. The data represent averages of 14−25 scans for each peptide sample and 2−4 scans for each model complex with data collection and reduction as described previously in detail.[31] In addition, data were also used from a library of Ni K-edge XAS data for model complexes with various ligation and coordination geometries that exist in the Stanford laboratory.

GNXAS Data Analysis. The data analysis was performed using the ab initio GNXAS method. The theoretical basis for the GNXAS approach and its fitting methodologies have been described in detail elsewhere.[32−34] The program code generates theoretical EXAFS signals based on an initial structural model. Cartesian coordinates for HC_4H_2 were obtained from an energy-minimized structure generated by the CHARMm program. For HC_5H, modifications were made to the structure of HC_4H_2 (utilizing Chem3D Pro) to generate new coordinates from assumed cobalt and nickel coordination modes. The coordinates were used as input to generate an initial structural model up to a distance cutoff of 5.0 Å. Phase shifts were calculated by using the standard muffin-tin approximation to calculate the individual two- and three-body EXAFS signals. A model EXAFS spectrum was constructed by combining the individual component signals and an appropriate background. This model was then fit to the averaged raw absorption data by a least-squares minimization program that uses the MINUIT subroutine of the CERN library. Background subtraction was performed by applying a flexible three-segment spline, which was refined in the GNXAS fits. The quality of the fit was calculated by the least-squares residual $\mathcal{R}$ and monitored through visual inspection of the fits to the

(26) Garnovskii, A. D.; Mistryukov, A. E.; Kochin, S. G.; Sergienko, V. S.; Vasil'chenko, I. S.; Porai-Koshits, M. A. *Mendeleev Commun.* **1991**, 110−111.
(27) Garnovskii, A. D.; Mistryukov, A. E.; Kochin, S. G.; Sergienko, V. S.; Vasil'chenko, I. S.; Minkina, L. S.; Porai-Koshits, M. A. *Russ. J. Inorg. Chem.* **1992**, *37*, 648−653.
(28) Yamamura, T.; Tadokoro, M.; Kuroda, R. *Chem. Lett.* **1989**, 1245−1246.
(29) El-Sayed, L.; El-Toukhy, A.; Iskander, M. F. *Transition Met. Chem.* **1979**, *4*, 300−305.
(30) Cramer, S. P.; Tench, O.; Yocum, M.; George, G. N. *Nucl. Instr. Methods A* **1988**, *266*, 586−591.
(31) DeWitt, J. G.; Bentsen, J. G.; Rosenzweig, A. C.; Hedman, B.; Green, J.; Pilkington, S.; Papaefthymiou, G. C.; Dalton, H.; Hodgson, K. O.; Lippard, S. J. *J. Am. Chem. Soc.* **1991**, *113*, 9219−9235.
(32) Filipponi, A.; Di Cicco, A.; Tyson, T. A.; Natoli, C. R. *Solid State Commun.* **1991**, *78*, 265−268.
(33) Filipponi, A.; Di Cicco, A.; Natoli, C. R. *Phys. Rev. B* **1995**, *52*, 15122−15134, ibid. 15135−15149.
(34) Westre, T. E.; Di Cicco, A.; Filipponi, A.; Natoli, C. R.; Hedman, B.; Solomon, E. I.; Hodgson, K. O. *J. Am. Chem. Soc.* **1995**, *117*, 1566−1583.

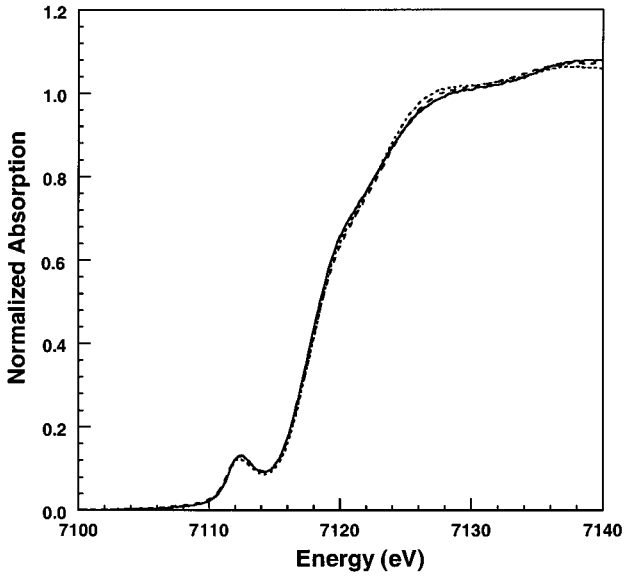

Figure 3. Normalized Fe K-edge spectra of HC_4H_2-$[Fe_4S_4]$-Ni (---), HC_5H-$[Fe_4S_4]$-Ni (•••), and the $[Fe_4S_4]^{2+}$ oxidation state of the nitrogenase Fe protein (—).[35] The data are almost entirely superimposable on one another, with respect to energies, shapes, and intensities for all of the observed transitions.

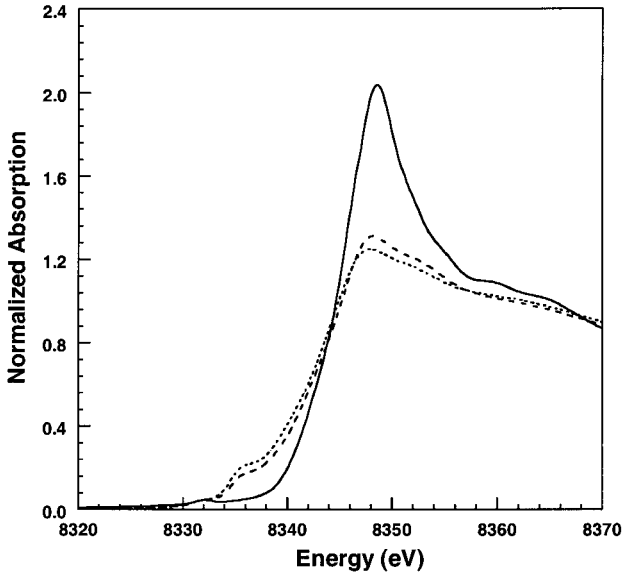

Figure 4. Normalized Ni K-edge spectra of $[Ni(OH_2)_6]Cl_2$ (—), HC_4H_2-$[Fe_4S_4]$-Ni (---), and HC_5H-$[Fe_4S_4]$-Ni (•••). Very large differences are seen between the edge spectra of the peptides and the starting material, $[Ni(OH_2)_6]Cl_2$, indicating that upon addition to the peptide, the ligation of Ni(II) has changed.

data and Fourier transform (FT) and the residual EXAFS signal and its FT. The structural parameters varied during the refinements were the bond distance (R) and the bond variance (σ_R^2). The nonstructural parameters E_0 and S_0^2 were varied, whereas the Γ_C (core hole lifetime) and E_r (experimental resolution) were kept fixed to physically reasonable values throughout the analysis. The coordination numbers were systematically varied in the course of the analysis, as discussed further in the EXAFS section; however, they were not allowed to float within a given fit. All parameters were varied within a preset range, and all results were checked to ensure that values obtained did not reach the high or low point of these fitting ranges. The Fe and Co data were fit over the k-range 3.5−17 Å^{-1} and the Ni data over the range 3.5−16 Å^{-1}. For HC_5H-$[Fe_4S_4]$-Co, the Fe K-edge data were truncated (k-range 3.5−12 Å^{-1}) at the onset of the Co K-edge.

Results and Discussion

Fe K-Edge XAS Data. (a) Fe K-Edges. The Fe K-edge spectra of HC_4H_2-$[Fe_4S_4]$-Ni and HC_5H-$[Fe_4S_4]$-M are almost entirely superimposable. The edges display the typical features of an Fe_4S_4 cluster of approximately tetrahedrally coordinated Fe atoms, with a prominent 1s → 3d preedge transition at ~7112 eV and a relatively featureless rising edge with a shoulder at ~7119 eV. The position of the edge is consistent with the $[Fe_4S_4]^{2+}$ cluster oxidation state.[35] As shown in Figure 3, the spectra are practically identical with that of the oxidized iron protein of nitrogenase and, by inference, to those of synthetic analogues known to contain $[Fe_4S_4]^{2+}$ clusters.

(b) Fe K-Edge EXAFS. As with the edge data, the EXAFS data of HC_4H_2-$[Fe_4S_4]$-Ni and HC_5H-$[Fe_4S_4]$-Ni are essentially superimposable to the end of the high k-range (17 Å^{-1}, data not shown). Excellent fits to the EXAFS data were obtained by assuming a typical cubane-type Fe_4S_4 structure, and the results are consistent with previous studies of $[Fe_4S_4]^{2+}$ clusters.[35] The best fits were achieved by using a coordination number of four for the Fe−S interaction at ~2.28 Å, and three for the Fe−Fe interaction at ~2.74 Å (for all samples the determined Fe−S and Fe−Fe distances were within ±0.01 Å of each other). The σ^2 parameters were small, and on the order expected for these cluster types. Despite the limited k-range available for HC_5H-$[Fe_4S_4]$-Co, analysis conclusively identified the presence of an $[Fe_4S_4]^{2+}$ cluster. On the basis of the edge and EXAFS data, the peptides do not appear to contain a mixture of species but rather one well-defined $[Fe_4S_4]^{2+}$ cluster structure.

Ni K-Edge XAS Data. (a) Ni K-Edges. In three of the four samples of HC_5H-$[Fe_4S_4]$-Ni, $[Ni(OH_2)_6]Cl_2$ was used as the Ni(II) source, whereas in the fourth $[Ni(OH_2)_6](BF_4)_2$ was used. The edge intensity and position, as well as the shape, number, and intensity of the edge transitions, are highly reproducible for the samples irrespective of the starting material used. This both demonstrates the reproducibility in sample preparation and eliminates the possibility that chloride is binding to Ni(II) upon addition to the peptide, information that is exceptionally useful for the EXAFS analysis, as described below. As seen in Figure 4, large differences exist between the edge spectra of the two Ni-peptides and the reactant $[Ni(OH_2)_6]Cl_2$, clearly indicating that the peptide-Ni interaction is causing a change in the Ni(II) ligation. The $[Ni(OH_2)_6]^{2+}$ spectrum contains a very weak 1s → 3d preedge feature (consistent with a near-octahedral geometry) followed by a very steep, featureless rising edge that reaches a maximum intensity of ~2.0 units at ~8348 eV. While the Ni-peptide spectra contain a preedge feature similar to that of $[Ni(OH_2)_6]Cl_2$, there is an additional feature superimposed along the rising edge centered around 8335 eV. This feature, which has been assigned as a 1s → $4p_z$ or 1s → 4p-plus-shakedown transition, is indicative of a square-planar geometry, with the intensity being a measure of the distortion from ideal symmetry.[36−38] The presence of this feature is highly diagnostic,

(35) Musgrave, K. B.; Angove, H. C.; Burgess, B. K.; Hedman, B.; Hodgson, K. O. *J. Am. Chem. Soc.* **1998**, *120*, 5325−5326.

(36) Cramer, S. P.; Eidsness, M. K.; Pan, W.-H.; Morton, T. A.; Ragsdale, S. W.; DerVartanian, D. V.; Ljungdahl, L. G.; Scott, R. A. *Inorg. Chem.* **1987**, *26*, 2477−2479.

(37) Colpas, G. J.; Maroney, M. J.; Bagyinka, C.; Kumar, M.; Willis, W. S.; Suib, S. L.; Baidya, N.; Mascharak, P. K. *Inorg. Chem.* **1991**, *30*, 920−928.

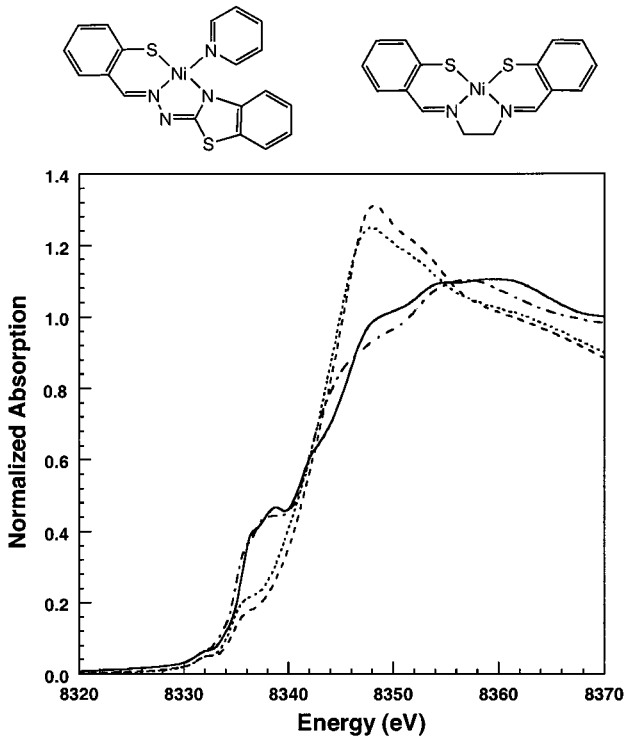

Figure 5. Normalized Ni K-edge spectra of HC_4H_2-[Fe_4S_4]-Ni (---), HC_5H-[Fe_4S_4]-Ni (···), a NiN_3S model complex (—), and a NiN_2S_2 model complex (· — · —). The model complex trends attributed to an increase in sulfur ligation are similar to the differences between the two metallopeptides, implying increased sulfur ligation in HC_5H-[Fe_4S_4]-Ni. The structures of the two model complexes are shown.

and thus indicates that a significant portion of the Ni(II) sites adopt a planar geometry.

The rising edges of the Ni-peptide spectra (Figure 4) occur at a lower energy and are neither as steep nor as intense, with a maximum edge intensity of ~1.3 and 1.2 units at ~8347 eV for HC_4H_2-[Fe_4S_4]-Ni and HC_5H-[Fe_4S_4]-Ni, respectively. There is an additional broader transition beyond the maximum at ~8352 eV. While a number of differences exist between [Ni-$(OH_2)_6$]Cl_2 and the peptides, the position and shape of the main edge transition at ~8347−8348 eV in both will prove useful in the further analysis.

There are less pronounced edge differences between the two Ni-peptides themselves. The transition around 8335 eV is somewhat more intense and better resolved in HC_5H-[Fe_4S_4]-Ni. While the edge position is shifted slightly to lower energy, the overall intensity is decreased and the transition around 8352 eV is less resolved in this peptide relative to HC_4H_2-[Fe_4S_4]-Ni.

It is instructive to compare the Ni-peptide data with edges of model complexes with known nitrogen/sulfur ligation. Relevant spectra are provided in Figure 5 for two complexes with planar stereochemistry.[26−28] Complexes with NiN_2S_2 and NiN_3S ligation demonstrate that with increased sulfur content there are minor changes, with the preedge position shifting somewhat to lower energy and the intensity decreasing. Both edges exhibit transitions above the rising edge. When comparing the Ni-peptide edges to those of the models, the transitions at 8335 eV are lower in intensity for the peptides, but the small energy shift and difference in intensity for the latter vs the

Table 1. Ni K-Edge GNXAS Fits to HC_4H_2-[Fe_4S_4]-Ni[a]

E_0	8335.4	8335.4	8335.4	8335.4
S_0^2	0.8	0.8	0.8	0.8
% $Ni(H_2O)_6$	20	20	30	40
R(Ni−O) (Å)	2.07	2.07	2.07	2.07
N[a]	1.2	1.2	1.8	2.4
σ^2 (Å^2)	0.0008	0.0009	0.0010	0.0029
R(Ni−N) (Å)	1.96	1.96	1.96	1.92
N[a]	2.4	1.6	2.1	1.8
σ^2 (Å^2)	0.0061	0.0044	0.0056	0.0028
R(Ni−S) (Å)	2.20	2.20	2.20	2.19
N[a]	0.8	1.6	0.7	0.6
σ^2 (Å^2)	0.0006	0.0023	0.0004	0.0003
$\mathscr{R}$ (fit)	0.104×10^{-6}	0.110×10^{-6}	0.106×10^{-6}	0.129×10^{-6}

[a] In the fits, the following parameters were refined: E_0, S_0^2, R(Ni−N, Ni−S), and the corresponding σ^2 values. The coordination numbers (N) were systematically varied but were not allowed to float in a given fit. The Ni−O distance was held constant at 2.07 Å in all of the fits. The Γ_c and experimental resolution parameters were fixed to physically reasonable values throughout the analysis. See text for definitions of the above-mentioned parameters.

Table 2. Ni K-Edge GNXAS Fits to the HC_5H-[Fe_4S_4]-Ni[a]

E_0	8335.4	8335.4	8335.4	8335.4
S_0^2	0.8	0.8	0.8	0.8
% $Ni(H_2O)_6$	20	20	30	40
R(Ni−O) (Å)	2.07	2.07	2.07	2.07
N[a]	1.2	1.2	1.8	2.4
σ^2 (Å^2)	0.0001	0.0009	0.0020	0.0069
R(Ni−N) (Å)	1.93	1.92	1.91	1.89
N[a]	2.4	1.6	1.4	1.2
σ^2 (Å^2)	0.0054	0.0036	0.0018	0.0016
R(Ni−S)	2.19	2.19	2.18	2.18
N[a]	0.8	1.6	1.4	1.2
σ^2 (Å^2)	0.0001	0.0012	0.0010	0.0006
$\mathscr{R}$ (fit)	0.128×10^{-6}	0.102×10^{-6}	0.103×10^{-6}	0.120×10^{-6}

[a] In the fits, the following parameters were refined: E_0, S_0^2, R(Ni−N, Ni−S), and the corresponding σ^2 values. The coordination numbers (N) were systematically varied but were not allowed to float in a given fit. The Ni−O distance was held constant at 2.07 Å in all of the fits. The Γ_c and experimental resolution parameters were fixed to physically reasonable values throughout the analysis. See text for definitions of the above-mentioned parameters.

NiN_3S/ NiN_2S_2 model ligation is consistent with an interpretation that there is a higher sulfur content in HC_5H-[Fe_4S_4]-Ni. Comparisons were also made to edge data of 5-coordinate complexes, which are characterized by a maximum in the 8345−8350 eV range and an unresolved shoulder on the rising edge.[37,38] Whereas some of the features could be interpreted in terms of 5-coordination, the EXAFS fit results (vide infra) eliminate this possibility, showing Ni−N (1.92−1.96 Å) and Ni−S (~2.20 Å) distances typical for Ni−N_2S_2/N_3S coordination (Tables 1 and 2). The Ni−N_3S_2 and Ni−N_2S_3 distances are typically longer, ~2.0 Å for Ni−N and >2.3 Å for Ni−S.[38]

Comparison of the peptide spectra to those of $[Ni(OH_2)_6]^{2+}$ and the model complexes clearly shows that similarities exist, suggesting that the peptides likely contain a mixture of two ligation modes. As the samples lose Ni(II) upon each sequential chromatographic purification, Ni(II) must be in equilibrium between a peptide-bound form and a peptide-free form. This equilibrium, which has been further corroborated by nickel binding studies,[39] would result in a mixture of Ni−O and Ni−N/S ligated sites. The most significant difference between the peptides and the model complexes is the strongly increased

(38) Tan, G. O. Ph.D. Thesis, Stanford University, 1993, Chapter 7.

(39) Laplaza, C. E.; Holm, R. H. *J. Biol. Inorg. Chem.* In press.

intensity of the main edge transition at ~8347 eV, which is close to the same energy as the ~8348 eV maximum of $[Ni(OH_2)_6]Cl_2$, suggesting that Ni(II) in the form of approximately octahedral $Ni-O_6$ (hereafter referred to as $[Ni(OH_2)_6]^{2+}$) is also present in the peptide samples. A mixture would furthermore have the effect of lowering on the absolute intensity scale for the ~8335 eV transitions indicative of a planar, mixed S/N geometry, which is consistent with the observed edge.

Two sets of edge simulations were performed in an attempt to quantify the amount of $[Ni(OH_2)_6]^{2+}$ present in the peptides. Simulated edge spectra were calculated by either systematically summing varying percentages of the respective NiN_3S or NiN_2S_2 and $[Ni(OH_2)_6]^{2+}$ spectra, or by subtracting a percentage of the $[Ni(OH_2)_6]^{2+}$ spectrum from the peptide data (in this case, the edge was renormalized after performing the subtraction). It should be noted that the model structures are not necessarily exactly those of the respective sites in the peptides, but it is assumed that the structural similarity, and thus spectral analogy, are such that the approach is valid. When the spectrum of HC_4H_2-$[Fe_4S_4]$-Ni is compared to a series of edge simulations containing varying percentages (in 10% increments) of NiN_3S + $[Ni(OH_2)_6]^{2+}$, the data are most similar to the edge comprised of 80% NiN_3S + 20% $[Ni(OH_2)_6]^{2+}$ as seen in Figure 6 (top panel). When the edge-maximum intensity is matched, the intensity of the ~8335 eV transition of the sum remains more pronounced than for the peptide. If a percentage of the $[Ni(OH_2)_6]^{2+}$ spectrum is subtracted from the peptide data and the edge renormalized (Figure 6, bottom panel), the 1 eV energy differential in the edge maximum causes an increasing trough at ~8349 eV, the ~8335 eV transition intensity is lower, and the ~8352 eV feature is reduced for the calculated spectrum. The overall combined limit for closest resemblance for these subtractions was for a 20−30% level of a $[Ni(OH_2)_6]^{2+}$-type site mixed with a NiN_3S binding site. Analogous simulations for HC_5H-$[Fe_4S_4]$-Ni were performed using the NiN_2S_2 model (Supporting Information) and the results are similarly consistent with the presence of 20−30% $[Ni(OH_2)_6]^{2+}$.

Based on the presence of the transitions at ~8335 eV, diagnostic of a square-planar geometry, and the peak maximum at ~8347−8348 eV, indicative of $[Ni(OH_2)_6]^{2+}$ ligation, and with the addition/subtraction approach described, the edge data thus demonstrate that the samples contain a mixture of $[Ni(OH_2)_6]^{2+}$ and metallopeptides containing Ni(II) coordinated in a distorted square-planar geometry with mixed nitrogen/sulfur ligation. Further comparisons with model complexes are consistent with an *increased* sulfur ligation in HC_5H-$[Fe_4S_4]$-Ni relative to HC_4H_2-$[Fe_4S_4]$-Ni.

(b) Ni K-Edge Fourier Transforms. There are two main peaks in the Fourier transforms (FTs) of the metallopeptide data shown in Figure 7. These are centered at ~1.4 and ~1.8 Å (nonphase shift corrected), with the first peak shifted to slightly higher *R* for HC_4H_2-$[Fe_4S_4]$-Ni. Based on comparisons with Ni−N/S model complexes, the position of the first peak corresponds primarily to Ni−N and the second to Ni−S interactions. The FT of $[Ni(OH_2)_6]^{2+}$ contains a single, intense peak centered at ~1.6 Å (not shown), which will interfere with both peaks in the metallopeptide FTs. If the amount of this species is similar in both metallopeptides, as indicated by the edge simulations, relative changes between the two FTs can still, however, identify

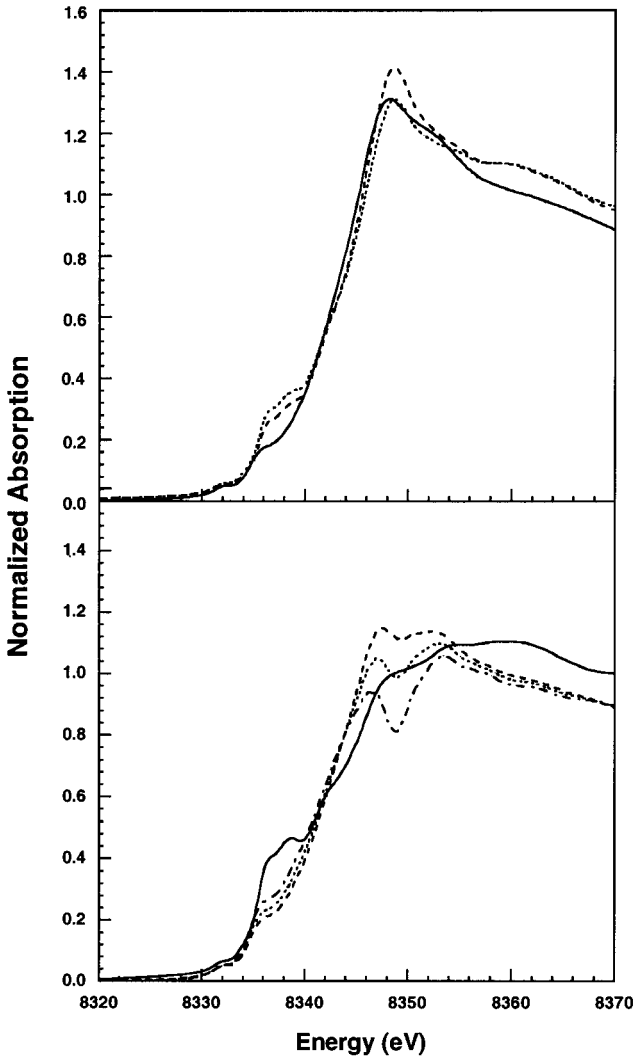

Figure 6. Comparison of simulated Ni K-edge spectra with that of HC_4H_2-$[Fe_4S_4]$-Ni. In the top panel, 70:30% (---) and 80:20% (···) of spectra of the NiN_3S model and of $[Ni(OH_2)_6]^{2+}$ are summed and compared to the peptide (—). In the bottom panel, varying percentages of the $[Ni(OH_2)_6]^{2+}$ spectrum are subtracted from the original peptide data. The spectra represent the subtractions −20% (---), −30% (···), and −40% (· − · −) as well as the unmodified NiN_3S model spectrum (—).

meaningful differences between the peptides. The most significant information provided by the FTs in Figure 7 is the 25% increased intensity of the second peak in HC_5H-$[Fe_4S_4]$-Ni relative to HC_4H_2-$[Fe_4S_4]$-Ni, indicating an increase in sulfur ligation, which is consistent with the edge analysis.

(c) Ni K-Edge EXAFS Analysis. Analyzing the EXAFS data of a mixture is challenging as the fitting parameters are correlated and the effect of small changes in coordination number are difficult to determine. It is clear from the edges and FTs that both peptides contain a mixture of Ni(II) sites. The edge simulations indicate approximately 20−30% $[Ni(OH_2)_6]^{2+}$ and 70−80% nitrogen/sulfur ligation, with the most probable assignments being NiN_3S and NiN_2S_2 for HC_4H_2-$[Fe_4S_4]$-Ni and HC_5H-$[Fe_4S_4]$-Ni, respectively. It is difficult, even under the best of circumstances, to determine accurately the coordination number of nitrogen in the presence of sulfur, and changes in coordination number are usually mainly manifested as a variation in the σ^2 parameters. A stronger focus was therefore put on determining the number of sulfur ligands. As

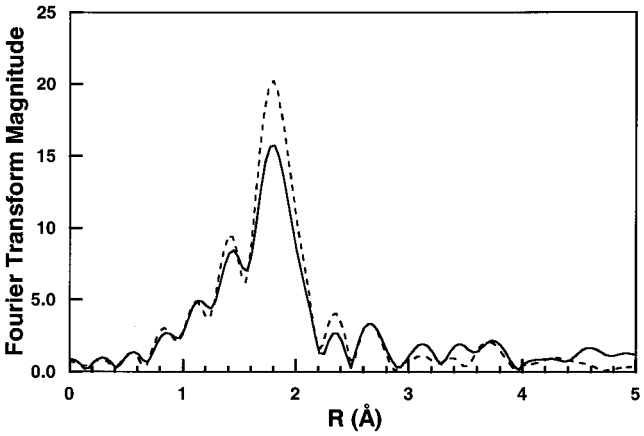

Figure 7. Comparison of nonphase shift corrected Ni EXAFS Fourier transforms of HC_4H_2-[Fe_4S_4]-Ni (—) and HC_5H-[Fe_4S_4]-Ni (---). In the latter, the peak at 1.8 Å has broadened and increased in intensity by ~25% relative to the former, indicating increased sulfur ligation to Ni(II).

the edge indicates that a significant portion of the Ni(II) is planar, the number of nitrogen ligands was derived from fixing the total coordination number as four. As previously mentioned, the XAS data for samples prepared with $[Ni(OH_2)_6]Cl_2$ or $[Ni(OH_2)_6](BF_4)_2$ as the Ni(II) source are identical. This result rules out chloride ligation, which would otherwise inhibit the ability to determine accurately the sulfur ligation, as sulfur and chlorine cannot be distinguished in the EXAFS analysis.

A systematic EXAFS analysis was undertaken in which either the ratio of the nitrogen/sulfur ligation or the percentage of $[Ni(OH_2)_6]^{2+}$ included in the fits was varied. To identify the number of sulfur ligands, fits were initially performed in which 20% $[Ni(OH_2)_6]^{2+}$ and varying nitrogen/sulfur ligation (for the remaining 80%) were tested. The coordination numbers were locked in a given fit but systematically varied between fits. Based on EXAFS fits of $[Ni(OH_2)_6]Cl_2$, the Ni−O distance was held constant at 2.07 Å. In fits to HC_4H_2-[Fe_4S_4]-Ni, when the sulfur coordination number was increased from 0.8 to 1.6 (80% of 1.0 and 2.0, respectively) a 4-fold increase, from 0.0006 Å^2 to 0.0023 Å^2, in the σ^2 parameter of the sulfur interaction resulted (Table 1). This was complemented by a less dramatic decrease in the σ^2 parameter of the nitrogen interaction as the coordination number was decreased from 2.4 to 1.6 (80% of 3.0 and 2.0, respectively). The large variations in the σ^2 parameters did not affect either of the distances. Varying the coordination numbers led to small but probably not statistically significant changes in the $\mathscr{R}$ value. However, as seen in Figure 8, the fit is visually better for the NiN_3S fits. When a similar set of fits was carried out for HC_5H-[Fe_4S_4]-Ni, they support the presence of two sulfur ligands (Table 2). In this case, the σ^2 parameter for the sulfur interaction is very low if only one sulfur ligand is included (0.0001 Å^2) and the fit also gives a very low σ^2 parameter for the $[Ni(OH_2)_6]^{2+}$ contribution. For two sulfurs, the σ^2(Ni−S) and σ^2(Ni−O) values increase to more realistic values (0.0012 and 0.0009 Å^2, respectively), and the $\mathscr{R}$ value decreases by 20%. Although the margins for difference in the fit results are low, it is clear that there is a mixture of ligations, with a slight preference for a higher sulfur content in HC_5H-[Fe_4S_4]-Ni, derived mainly from the σ^2 values.

A second set of fits were performed in which the nitrogen/sulfur ligation was held at optimal values as determined in the previous fits, while the percentage of $[Ni(OH_2)_6]^{2+}$ was varied

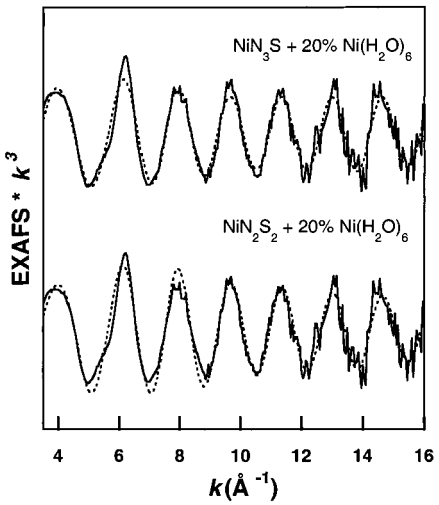

Figure 8. Comparison of the total Ni EXAFS signal (---) compared with the experimental EXAFS data (—) for fits to HC_4H_2-[Fe_4S_4]-Ni with either N_3S (top) or N_2S_2 (bottom) ligation in addition to 20% $[Ni(OH_2)_6]^{2+}$.

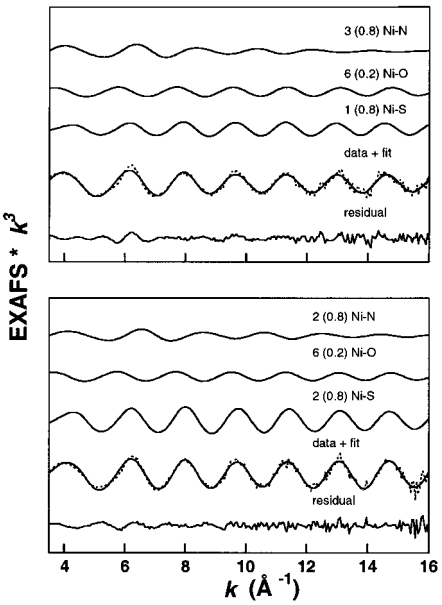

Figure 9. Individual Ni EXAFS contributions and the total Ni EXAFS signal (—) compared with the experimental EXAFS data (---) for HC_4H_2-[Fe_4S_4]-Ni (top panel) and HC_5H-[Fe_4S_4]-Ni (bottom panel). The Ni−N, Ni−O, and Ni−S coordination numbers have been adjusted to account for the presence of 20% $[Ni(OH_2)_6]^{2+}$.

between 20 and 40%. For HC_4H_2-[Fe_4S_4]-Ni (using NiN_3S ligation), nearly identical fits were obtained when 20% or 30% $[Ni(OH_2)_6]^{2+}$ is assumed. The 20% fit (Figure 9, top panel) contains 2.4 Ni−N, 1.2 Ni−O, and 0.8 Ni−S interactions at 1.96, 2.07, and 2.20 Å, respectively. As would be predicted, the effect is seen in the σ^2 parameters. When 40% $[Ni(OH_2)_6]^{2+}$ is included, there is an increase in the $\mathscr{R}$ value, the Ni−N distance becomes shorter, and the σ^2 parameter for the Ni−O wave triples. As shown in Table 2, similar results are seen in fits to HC_5H-[Fe_4S_4]-Ni, with inclusion of 20−30% $[Ni(OH_2)_6]^{2+}$ again leading to the most reasonable fits. The fit with 20% is shown in Figure 9 (bottom panel), with 1.6 Ni−N at 1.92 Å, 1.2 Ni−O at 2.07 Å, and 1.6 Ni−S at 2.19 Å. As for HC_4H_2-[Fe_4S_4]-Ni, the fits become worse when the amount of $[Ni(OH_2)_6]^{2+}$ is 40% or higher, and the Ni−N distance becomes shorter.

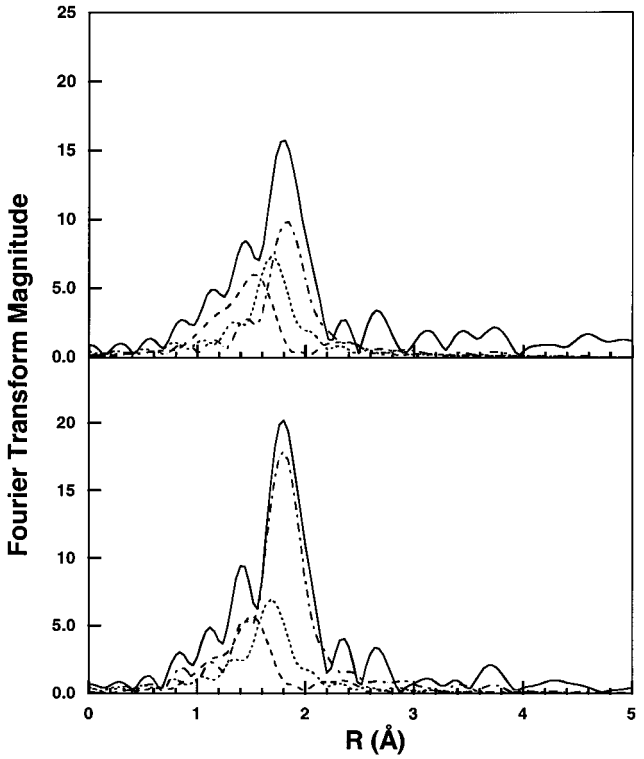

Figure 10. Deconvolution of the nonphase shift corrected Ni EXAFS Fourier transforms of HC_4H_2-[Fe_4S_4]-Ni (top panel) and HC_5H-[Fe_4S_4]-Ni (lower panel). The data (—) and the Ni−N (---), Ni−O (···), and Ni−S (· − · −) contributions are shown. A much larger Ni−S contribution is seen for HC_5H-[Fe_4S_4]-Ni.

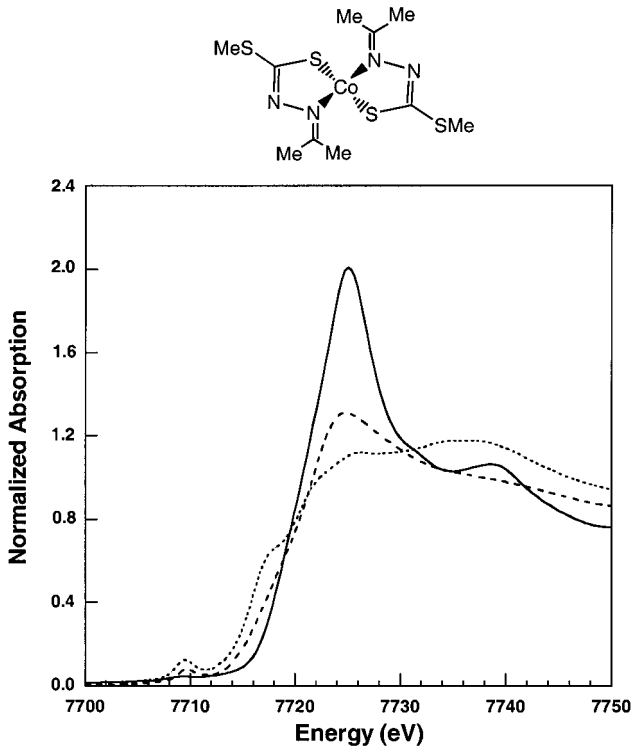

Figure 11. Normalized Co K-edge spectra of $[Co(OH_2)_6](BF_4)_2$ (—), HC_5H-[Fe_4S_4]-Co (---), and the indicated CoN_2S_2 model complex (···). Significant differences are seen between the edge spectra of the metallopeptide and the starting material, $[Co(OH_2)_6](BF_4)_2$, indicating that upon reaction with the peptide, the ligation of Co(II) has changed.

The EXAFS fit deconvolutions (Figure 9) reveal that the Ni−N and Ni−O waves are ∼180° out of phase with each other, leading to a cancellation of the resulting signal and reducing significantly their combined contribution to the EXAFS wave. The sulfur contribution will therefore dominate the overall EXAFS signal even more than first expected. The FT deconvolutions displayed in Figure 10 clearly show the larger Ni−S contribution in HC_5H-[Fe_4S_4]-Ni (bottom panel). The differences between the respective Ni−N and Ni−O contributions are not as significant.

Co K-Edge XAS Data. (a) Co K-Edges. As with the Ni-containing peptides, significant differences are seen when $[Co(OH_2)_6](BF_4)_2$ and HC_5H-[Fe_4S_4]-Co are compared in Figure 11, indicating that upon addition to the peptide, the ligation of Co(II) changes. The steep featureless rising edge of the $[Co(OH_2)_6]^{2+}$ spectrum is similar in shape and overall intensity (∼2.0 units) to that of $[Ni(OH_2)_6]^{2+}$. In the peptide data, an intense preedge feature that was not present in $[Co(OH_2)_6](BF_4)_2$ is seen at 7710 eV. This feature is assigned as a formally dipole-forbidden 1s → 3d transition, which derives intensity mainly from electric dipole 3d−4p mixing and to a small extent from electric quadrupole coupling. A high degree of 3d−4p mixing occurs in noncentrosymmetric sites, particularly those with tetrahedral geometry.[40−42] Thus, the high intensity of the preedge transition strongly indicates that a significant portion of Co(II) in the peptide sample has adopted a tetrahedral geometry. The rising edge of the peptide is neither as intense nor as steep as the starting material, rising to a maximum intensity of ∼1.3 units, with an energy near 7725 eV for both.

Data for a tetrahedral CoN_2S_2 model complex were also measured (Figure 11). The edge for HC_5H-[Fe_4S_4]-Co, although similar in shape, is less featured than that of the model. A lack of extensive Co(II) model data limits further edge comparisons to other ligation modes and coordination geometries. Edge simulations for HC_5H-[Fe_4S_4]-Co, carried out in an analogous manner to those for the Ni peptides, resulted in a distribution of 20−30% $[Co(OH_2)_6]^{2+}$ and 70−80% of peptide-bound Co(II).

(b) Co K-Edge Fourier Transforms and EXAFS Analysis. The FT of the peptide provided in Figure 12 contains two peaks centered at ∼1.5 and ∼1.9 Å, with an intensity ratio of ∼1:2. This compares favorably with the FT of the CoN_2S_2 model complex (not shown). An EXAFS analysis approach similar to that for the Ni(II) peptides was used. Initially, fits were attempted in which three contributions, Co−N, Co−O, and Co−S, were included. The Co−N and Co−O distances refined to values that were too close in distance to be resolvable within the data range, as defined by $\Delta R = \pi/2\Delta k$. When the Co−N and Co−O interactions were included as a single contribution, the distance refined to 2.05 Å. A series of systematic fits are given in Table 3, and for 20% $[Co(OH_2)_6]^{2+}$ included 2.8 Co−N/O interactions at 2.05 Å and 1.6 Co−S interactions at 2.26 Å. That fit is given in Figure 13. The Co−N/O coordination number was assigned as 0.80(2 N) + 0.20(6 O) and the Co−S coordination number as 0.80(2 S). The combined results of the edge, FT, and EXAFS analysis support a tetrahedral Co−N_2S_2 environment.

(40) Shulman, R. G.; Yafet, Y.; Eisenberger, P.; Blumberg, W. E. *Proc. Natl. Acad. Sci. U.S.A.* **1976**, *73*, 1384−1388.
(41) Bair, R. G.; Goddard, W. A. *Phys. Rev. B* **1980**, *22*, 2767−2776.
(42) Westre, T. E.; Kennepohl, P.; DeWitt, J. G.; Hedman, B.; Hodgson, K. O.; Solomon, E. I. *J. Am. Chem. Soc.* **1997**, *119*, 6297−6314.

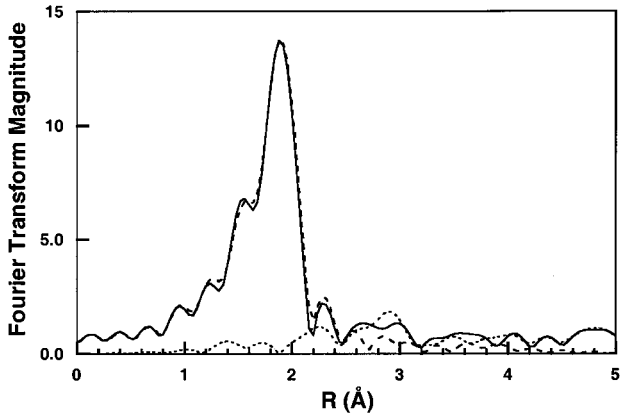

Figure 12. Nonphase shift corrected Co EXAFS Fourier transforms of the experimental data (—) vs the fit signals (---) for HC_5H-[Fe_4S_4]-Co. The Fourier transform of the EXAFS fit residual (•••) is also shown.

Table 3. Co K-Edge GNXAS Fits to HC_5H-[Fe_4S_4]-Co[a]

E_0	7721.1	7721.5	7721.2	7721.0
S_0^2	0.8	0.8	0.8	0.8
% $Co(H_2O)_6$	10	20	30	40
R(Co−N/O) (Å)	2.05	2.05	2.07	2.06
N[a]	2.4	2.8	3.2	3.6
σ^2 (Å^2)	0.007	0.007	0.010	0.014
R(Co−S) (Å)	2.26	2.26	2.26	2.26
N[a]	1.8	1.6	1.4	1.2
σ^2 (Å^2)	0.002	0.001	0.001	0.001
$\mathscr{R}$ (fit)	0.42×10^{-7}	0.41×10^{-7}	0.40×10^{-7}	0.40×10^{-7}

[a] In the fits, the following parameters were refined: E_0, S_0^2, R(Co−N/O, Co−S), and the corresponding σ^2 values. The coordination numbers (N) were systematically varied but were not allowed to float in a given fit. The Γ_c and experimental resolution parameters were fixed to physically reasonable values throughout the analysis. See text for definitions of the above-mentioned parameters.

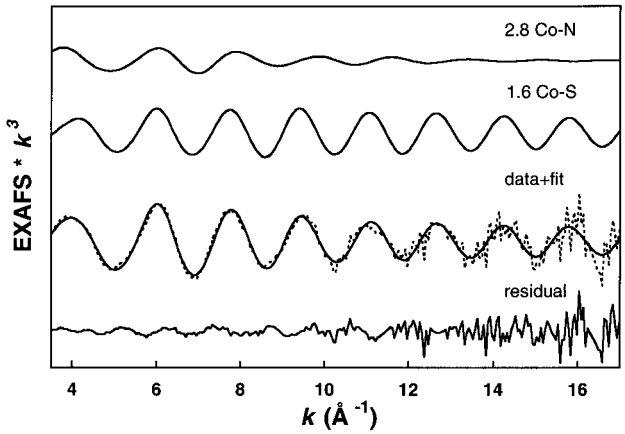

Figure 13. Individual Co EXAFS contributions and the total Co EXAFS signal (—) compared with the experimental EXAFS data (---) for HC_5H-[Fe_4S_4]-Co. The Co−N/O and Co−S coordination numbers have been adjusted to account for the presence of 20% $[Ni(OH_2)_6]^{2+}$.

Conclusions

The Fe K-edge and EXAFS data clearly establish the presence of a cubane-type Fe_4S_4 cluster in the metallopeptides HC_4H_2-[Fe_4S_4]-Ni and HC_5H-[Fe_4S_4]-M (M = Ni(II), Co(II)), a result consistent with absorption spectra and metal analysis.[19] The Ni and Co K-edge data indicate that the peptide samples are comprised of a mixture of $[M(OH_2)_6]^{2+}$ and either distorted square-planar Ni(II) or tetrahedral Co(II) with mixed nitrogen/sulfur ligation. Based on edge simulations, in which results from close but not necessarily identical sites in model complexes were used, the data are most consistent with the presence of 20−30% $[M(OH_2)_6]^{2+}$ and 70−80% of the anticipated nitrogen/sulfur ligation. This was further supported by EXAFS analyses, in which either the N:S ratio or the percentage of $[M(OH_2)_6]^{2+}$ included in the fits was varied. The best fit in each case was obtained with 20−30% $[M(OH_2)_6]^{2+}$ and 70−80% of the designed nitrogen/sulfur ligation. When 40% or more $[M(OH_2)_6]^{2+}$ was included in the fits, they became significantly worse. These concentrations of $[M(OH_2)_6]^{2+}$ are also consistent with those predicted by nickel equilibrium binding results.[39] For instance, based on the site binding constants ca. 25% of the nickel in the HC_4H_2-[Fe_4S_4]-$Ni_{0.8}$ sample is expected to exist in the form of $[Ni(OH_2)_6]^{2+}$.

The presence of $[M(OH_2)_6]^{2+}$ in the peptide samples provides limitations to the fits of the Ni and Co K-edge and EXAFS data; however, as summarized above, it was still possible to obtain a structural picture of the metal sites. There is a more subtle indication in fit parameters due to high correlation, but strongly supported by the Fourier transform and to a lesser degree by the edge data, that the sulfur ligation is increased in HC_5H-[Fe_4S_4]-Ni relative to HC_4H_2-[Fe_4S_4]-Ni. Assuming a mixture of $[M(OH_2)_6]^{2+}$ and N/S ligation, excellent fits to the EXAFS data were achieved. The XAS analysis thus strongly suggests that the peptides contain the desired preformed metal binding sites.

XAS investigations have been reported for CODH from *Clostridium thermoaceticum*,[36,43,44] which in addition to the A-Cluster, contains the C-Cluster, another spectroscopically deduced [Ni-X-Fe_4S_4] assembly that differs from the A-Cluster in the ligand environment around the nickel atom. Especially pertinent to this work are the XAS studies by Scott and coworkers[21,22] on the isolated α-subunit inasmuch as it contains only the A-Cluster. It is important to recognize, however, that the A-Cluster can exist as a Ni-labile or a Ni-nonlabile form, the Ni-labile site being the only one with activity.[45] The K-edge and EXAFS studies on this mixture[21] indicate an average environment for all nickel sites of 2 N/O ligands at 1.89 Å and 2 S ligands at 2.19 Å in a distorted square-planar environment. The XAS of the Ni-nonlabile sites[22] indicate a slightly more distorted square-planar coordination than in the mixture, with Ni(II) coordinated to 2 N/O ligands at 1.87 Å and 2 S ligands at 2.20 Å. Unfortunately, at this point it is not possible to isolate the Ni-labile sites. It is still interesting, however, to compare the data on the homogeneous Ni-nonlabile sites of CODH with that of the metallopeptides, in particular HC_5H-[Fe_4S_4]-Ni, which was designed to have N_2S_2 ligation similar to the A-Cluster of the protein. As discussed, the metallopeptide fitting results are not straightforward because of the presence of $[Ni(OH_2)_6]^{2+}$. After removing 20% of $[Ni(OH_2)_6]^{2+}$, the edge of HC_5H-[Fe_4S_4]-Ni (Figure 5) compares reasonably well with that of the protein data (cf. Figure 1 of ref 22). The edges of both contain three transitions at about the same energies and with similar intensities, one on the rising edge at 8338 eV and two fairly resolved peaks at 8346 and 8352 eV. The ratio of the two peaks in the FT of the protein and HC_5H-[Fe_4S_4]-Ni are

(43) Bastian, N. R.; Diekert, G.; Niederhoffer, E. C.; Teo, B.-K.; Walsh, C. T.; Orme-Johnson, W. H. *J. Am. Chem. Soc.* **1988**, *110*, 5581−5582.
(44) Ralston, C. Y.; Wang, H.; Ragsdale, S. W.; Kumar, M.; Spangler, N. J.; Ludden, P. W.; Gu, W.; Jones, R. M.; Patil, D. S.; Cramer, S. P. *J. Am. Chem. Soc.* **2000**, *122*, 10553−10560.
(45) Xia, J.; Hu, Z.; Popescu, C. V.; Lindahl, P. A.; Münck, E. *J. Am. Chem. Soc.* **1997**, *119*, 8301−8312.

again similar. The slightly higher intensity of the second peak in HC_5H-[Fe_4S_4]-Ni may be attributable to the presence of Ni−O (in the form of $[Ni(OH_2)_6]^{2+}$) contributing to the intensity of this peak. The EXAFS data and fit results for the protein and HC_5H-[Fe_4S_4]-Ni are also similar. While direct comparisons cannot be made, owing to the presence of $[Ni(OH_2)_6]^{2+}$ in HC_5H-[Fe_4S_4]-Ni, the σ^2 parameters of the Ni−N and Ni−S interactions are similar (0.0039 and 0.0036 for the Ni−N and 0.0019 and 0.0012 Å^2 for the Ni−S interactions in the protein[22] and the metallopeptide, respectively), implying an equal amount of disorder in both. The Ni−N distances are longer in both HC_4H_2-[Fe_4S_4]-Ni and HC_5H-[Fe_4S_4]-Ni (1.92 and 1.96 Å, compared with 1.87 Å for the protein), while the Ni−S distances (2.20 Å) are the same in all cases. Finally, that no positive indication of a Ni/Co−Fe interaction was found in the metallopeptides is not surprising. Among all the XAS studies on CODH, only one[43] has been able to accommodate an interaction that could possibly arise from Ni−Fe scattering.

The collective XAS results for HC_4H_2-[Fe_4S_4]-Ni and HC_5H-[Fe_4S_4]-M demonstrate the presence of an Fe_4S_4 cluster and support the existence of the distorted square-planar coordination units $[Ni^{II}(S{\cdot}Cys)(N{\cdot}His)_3]$ and $[Ni^{II}(S{\cdot}Cys)_2(N{\cdot}His)_2]$ in the HC_4H_2 and HC_5H metallopeptides, respectively. We conclude that the designed binding sites, with Cys-26 as the bridging ligand, have been achieved; structural results are presented in Figure 2. This is the first XAS study of a *de novo* designed metallopeptide intended to stabilize a bridged biological assembly. In this and earlier work, we have selected the spectroscopically deduced structure of A-Cluster as an objective with which to address the scaffolding concept. Because the X-ray structure of CODH is not yet available,[46] we do not describe the bridged assemblies as structural analogues of the native sites. More significant is the demonstration of the scaffolding concept itself, which should be extendable to other sites.

Acknowledgment. This research was supported by NIH grants GM 28856 (to R.H.H.) and RR 01209 (to K.O.H.). The Stanford Synchrotron Radiation Laboratory is supported by the Department of Energy, Office of Basic Energy Sciences. The SSRL Structural Molecular Biology Program is supported by the National Institutes of Health, National Center for Research Resources, Biomedical Technology Program, and the DOE Office of Biological and Environmental Research. C.E.L. has held a Harvard Graduate School of Arts and Sciences Graduate Prize Fellowship and a National Science Foundation Minority Graduate Fellowship. A significant portion of data in our nickel K-edge XAS library was provided by Professor R. A. Scott, University of Georgia.

Supporting Information Available: Comparison of observed and simulated Ni K-edge spectra of HC_5H-[Fe_4S_4]-Ni alone and with varying proportions of $[Ni(OH_2)_6]^{2+}$, and the observed spectrum of a distorted planar NiN_2S_2 model compound (PDF). This material is available free of charge via the Internet at http://pubs.acs.org.

JA011861Q

(46) While this manuscript was under review, two reports of the structure of the C-cluster of CODH from different organisms were published. In *Carboxydothermus hydrogenoformans* CODH (1.6 Å resolution), the active center has the $NiFe_4S_5$ composition in which the nickel atom is bonded to two sulfur atoms of a cuboidal Fe_3S_4 and bridged through a Ni−S−Fe interaction to an iron atom external to this fragment (Dobbek, H.; Svetlitchnyi, V.; Gremer, L.; Huber, R.; Meyer, O. *Science* **2001**, *293*, 1281−1285). In *Rhodospirillum rubrum* CODH (2.8 Å resolution), the center appears to contain a cubane-like $NiFe_3S_4$ unit to which an iron atom is bridged through a cysteinyl sulfur atom and a sulfur atom of the cubane-like unit (Drennan, C. L.; Heo, J.; Sintchak, M. D.; Schreiter, E.; Ludden, P. W. *Proc. Natl. Acad. Sci. U.S.A.* **2001**, *98*, 11973−11978).